# Preface

Alzheimer's disease (AD), a common neurodegenerative disorder, was first reported by the German psychiatrist Alois Alzheimer in the year 1906. It is a progressive neurodegenerative disorder, primarily characterized by dementia and cognitive impairment. More than 80% of dementia cases worldwide, in older people, were featured by the deposition of amyloid β and neurofibrillary tangles. The global burden on the population suffering from AD was assessed to 44 million in 2015. This number is expected to double by 2030 and triple by 2050, if no effective treatment is in place. In a country like India, where approximately 41% of the population is in the age group of 30 to 55 years, AD needs to be sincerely acknowledged and addressed. Several targets of the disease have been reported including acetylcholinesterase (AChE), butyrylcholinesterase (BuChE), monoaminoxidase-B (MAO-B), β-secretase, γ-secretase, β-site APP cleaving enzyme-1 (BACE-1), NMDA receptors, matrix metalloproteinases (MMPs), tau-tubulin kinase (TTBK), muscarinic acetylcholine receptor, nicotinergic acetylcholine receptor, *etc*. In spite of decades of study on the etiology of disease and also the significant efforts by various pharmaceutical industries to develop therapies, there is no effective treatment available to cure AD or to inhibit its progression. However, there are three drugs (*viz.* donepezil, galantamine, and rivastigmine) as cholinergic enhancers, approved by USFDA. The latest (2003) approved drug memantine acts on N-methyl-D-aspartate (NMDA) receptor. The complex and multifactorial nature of the disease necessates to develop small multifunctional molecules as a better option for the treatment of AD.

The development of multifactorial leads with the ability to provide symptomatic relief along with modulation of pathogenic factors, *i.e*., cholinergic transmission, neuroinflammation, oxidative stress, TTBK-1 and MMPs, is the central goal of the present study. The work has been divided into six chapters. Chapter 1 deals with different types of neurodegenerative disorders, pathophysiology, diagnosis of AD and available treatments.

Chapter 2 deals with identification of selective matrix metalloproteinase-9 inhibitors with cholinesterase inhibition. These were identified by using combined structure-based and ligand-based drug design approaches, following molecular dynamic (MD) simulation. Structure-based pharmacophores were developed from five protein

structures of MMP-9 collected from RCSB. An equal number of e-pharmacophores were developed from refined crystal structures by Glide, Schrödinger suite 2015-1 and were validated by Güner-Henry scoring method. Ligand-based pharmacophores were developed by utilizing known MMP-9 inhibitors collected from literature and BindingDB site. They were selected based on higher Canvas similarity concerning N-isobutyl-N-(4-methoxyphenyl sulfonyl)glycyl hydroxamic acid (NNGH) as reference. Three 3D-QSAR models were developed using Phase, Schrödinger suite 2015-1 and validated internally (by PLS analysis) and externally. Developed pharmacophore matched molecules were screened out from 'Zinc15' database compounds. The final hits were collected after removal of pan-assay interference compounds (PANS), high-throughput virtual screening (HTVS), molecular docking and physiochemical properties prediction. The selected hits were purchased for *in vitro* MMP-9 inhibition studies along with blood-brain barrier (BBB) permeability, cell viability and neuroprotection studies to establish the *in silico* findings. The obtained hits from the study were attractive MMP-9 inhibitors with IC_{50} values of 81.22±0.23 nM, 122.98±0.15 nM, 242.92±0.12 nM, 277.61±0.12 nM (ZINC23114578, ZINC21212924, ZINC09613137, and ZINC06455433 respectively).
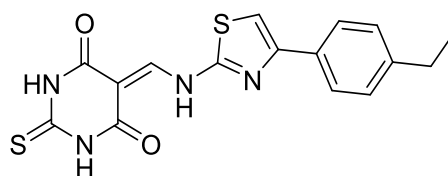
ZINC23114578

MMP-9, IC_{50}= 81.22±0.23 nM

AChE, IC_{50}= 643.2±0.058 nM

BuChE, IC_{50}= 65026±0.24 nM

Propidium displacement (3 μM)=100%

PAMPA, Pe(10^{-6} cm s^{-1})= 8.055±0.67, CNS+

In another study included in Chapter 3, peripheral anionic site (PAS) selective AChE inhibitors were identified by utilizing combined structure-based and ligand-based drug design approaches with MD simulation. PAS selective AChE inhibitors were obtained from 'Zinc15' database compounds using known AChE inhibitors and crystal structures of AChE. The identified hits showed PAS selective AChE inhibition (Ki value) within the nanomolar range (0.21±0.027 μM, 0.27±0.064 μM, 0.3±0.018 μM, and 0.28±0.032 μM for ZINC20592007, ZINC05354646, ZINC20649934, and

ZINC39154782 respectively). The hits also had good BBB permeability and neuroprotective activity against L-glutamate induced excitotoxicity. Further, the hits were non-toxic against neuroblastoma SH-SY5Y cell.
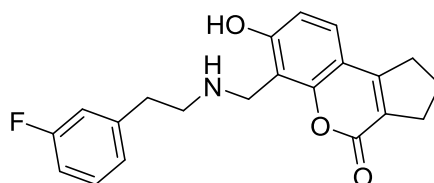

ZINC20592007

AChE, IC_{50}= 482±1.88 nM
BuChE, IC_{50}= 23954±5.69 nM
Propidium displacement (3μM)=100%
PAMPA, Pe(10^{-6} cm s^{-1})= 5.7±0.20, CNS+

In Chapter 4, the third target selected for the hits identification TTBK-1 is included. Structure-based pharmacophores integrated with MD simulations afforded ZINC14644839, ZINC00012956, ZINC91332506, and ZINC69775110 as novel human TTBK1 inhibitors. Hits produced stable hydrogen bonding interactions with Gln110, Gly111, Glu77, Asn113, and Asp176; similar to TTBK1 inhibitor 2KC (Gln110, Asp176, Asn159, and Glu77) and had remarkable drug-likeness properties.
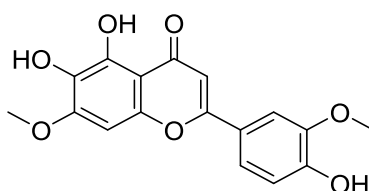

ZINC14644839

Glide docking score= -10.71 kcal/mole
IFD docking score= -11.29 kcal/mole

Chapter 5 contains synthesis and evaluation of 4-oxo-N, 4-diphenylbutan amides and E-N-aryl-4-hydroxy-4-phenylbut-2-enamides as anti-Alzheimer's agents. 4-Oxo-N, 4-diphenylbutanamides were identified as inhibitors of MAO-B and AChE through fragment-based drug design. The designed molecules were synthesized and characterized by ^{1}H NMR, ^{13}C NMR, and MASS spectral analysis and *in vitro* enzyme inhibition studies were performed against MAO-A, MAO-B, AChE, and BuChE. Among the synthesized compounds, compound **6m** (IC_{50} value 11.537±0.064 nM) produced most potent MAO-B inhibition.

6m
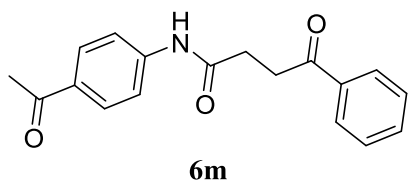
MAO-B, IC_{50}= 11.537±0.064 nM

MAO-A, IC_{50}= 76.986±0.071 nM

AChE, IC_{50}= 1.221±0.47 μM

BuChE, IC_{50}= 49.93±0.829 μM

Pe(10^{-6}cm s^{-1})= 9.63±0.23, CNS+

6p
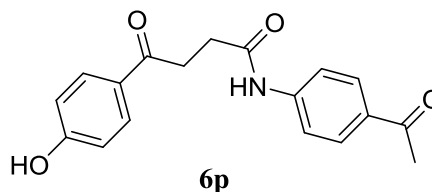
MAO-B, IC_{50}= 25.194±0.017 nM

MAO-A, IC_{50}= 37.212±0.4 nM

AChE, IC_{50}= 0.691±0.43 μM

BuChE, IC_{50}= 58.75±1.25 μM

Pe(10^{-6}cm s^{-1})= 11.35±0.28, CNS+

Electron withdrawing groups (*e.g.,* CF$_3$, COMe) at *meta*-position of N-phenyl was prominent for the potent activity as compared to *para*-substitution in 4-oxo-N, 4-diphenylbutanamides**.** Further, substitution at *para*-OH in 4-phenyl moiety of E-N-aryl-4-hydroxy-4-phenyl but-2-enamides showed better inhibition activity than other groups (*i.e*., H, CH$_3$, Cl, OMe).

E-N-Aryl-4-hydroxy-4-phenylbut-2-enamides were identified as inhibitors of MAO, MMP-9 and cholinesterase through fragment-based drug design. The designed molecules were synthesized and characterized by comprehensive spectral analysis. The *in vitro* enzyme inhibition studies were performed against MAO-A, MAO-B, AChE, BuChE, and MMP-9. Among the synthesized compounds, compounds **7k**, **7u**, and **7v** (IC_{50} values 3.178±0.02, 3.863±0.17, and 5.270±0.13 nM respectively) produced most potent MAO-B inhibition, however compound **7v** had moderate BBB permeability.
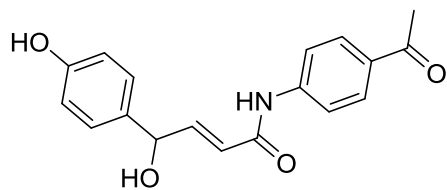

7k
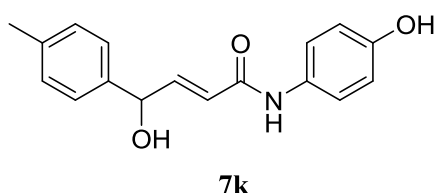
MAO-B, IC_{50}= 3.178±0.02 nM

MAO-A, IC_{50}= 6.222±0.19 nM

AChE, IC_{50}= 0.952±0.26 μM

BuChE, IC_{50}= 32.363±0.21μM

Pe(10^{-6}cm s^{-1}) =4.19±0.14, CNS+

7u
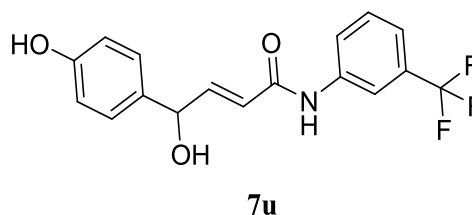
MAO-B, IC_{50}= 3.863±0.17 nM

MAO-A, IC_{50}= 11.229±0.04 nM

AChE, IC_{50}= 0.734±0.20 μM

BuChE, IC_{50}= 22.863±0.36 μM

Pe(10^{-6}cm s^{-1}) = 5.81±0.39, CNS+

6-Quinolyl amide, compound **7p** showed potent MMP-9 inhibition activity (IC_{50} value 167.2±0.074 nM) along with MAO-B and AChE inhibition.

7v

MAO-B, IC_{50}= 5.270±0.13 nM
MAO-A, IC_{50}= 23.662±0.07 nM
AChE, IC_{50}= 0.989±0.15 μM
BuChE, IC_{50}= 31.408±0.39 μM
Pe(10^{-6}cm s^{-1}) = 2.20±0.048, CNS+
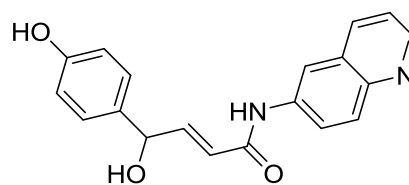
7p

MAO-B, IC_{50}= 6.953±0.072 nM
MAO-A, IC_{50}= 28.725±0.053 nM
MMP-9, IC50= 167.2±0.074 nM
AChE, IC_{50}= 1.525±0.11 μM
BuChE, IC_{50}= 20.782±0.21 μM
Pe(10^{-6}cm s^{-1}) = 3.77±0.4, CNS+

The relevant references have been included at the end of each chapter.

The summary and prespective of the study have been presented in Chapter 6, which is followed the Appendix.

———————